Graphene-modulated interfacial exchange coupling across organic molecular/ferromagnet spin interfaces

Yu Wang, Zheng Wang, and Xiaoguang Li*
Institute for Advanced Study, Shenzhen University, Shenzhen 518060, China

(Received 1 August 2023; revised 28 November 2023; accepted 10 January 2024; published 26 January 2024)

Magnetic molecules on ferromagnetic metallic substrates have been widely explored to exploit the potential for molecular magnetic storage and spintronics applications. Recent advances in these hybrid interfaces integrated with two-dimensional materials have been proposed as a flexible platform for realizing new spin-related effects. Herein, the impact of inserting graphene on the electronic and magnetic properties of a family of transition metal phthalocyanines (TMPcs, TM = Cr, Mn, Fe, Co, and Cu) deposited on ferromagnetic Ni(111) surfaces have been systematically rationalized by density functional theory analysis. Our calculations reveal that the magnetic exchange interaction across the molecule-substrate interfaces can be significantly mediated by the introduction of a graphene interlayer. Interestingly, these TMPcs exhibit ferromagnetic coupling with the Ni substrate. However, the strength of this coupling is reduced in the presence of a graphene decoupling layer, with the exception of CoPc. In the case of CoPc, the original ferromagnetic coupling with Ni(111) can be altered to antiferromagnetic when a graphene interlayer is introduced. By analyzing the different channels of communication involved in the spin interaction between the molecule and the magnetic substrate, we attribute these significant differences to the varied influences on the exchange interaction caused by the intermediary graphene layer. The presence of the inserted graphene layer may block the direct exchange interaction between the TMPc molecule and substrate, while the indirect superexchange interaction facilitated by the nitrogen atoms of the organic ligands is only reduced. Our study thus demonstrates that the inserted graphene can serve as an optimal intermediary layer for mediating the magnetic couplings across the molecule-substrate interfaces while allowing effective spin communication between them. These findings provide important insights into relevant experiments and offer a promising strategy to control the magnetic exchange interactions via utilizing graphene at metal-molecule interfaces.

DOI: 10.1103/PhysRevB.109.014428

I. INTRODUCTION

Molecular spintronics has attracted considerable attention due to interest from the viewpoints of both fundamental research and potential technological application [1–6]. In the last decade, new insights in the fundamental phenomena of hybrid interfaces formed by molecules adsorbed on magnetic surfaces are presenting a new pathway for developing the subfield of interface-assisted molecular spintronics—molecular spinterface [7–12]. Molecular materials play a crucial role in the development of a new generation of spin-based applications such as information storage devices [13,14], sensor [15], and quantum computing [16,17]. Among these materials, organometallic molecules comprising transition metal (TM) centers with localized d states are considered to be a promising class of candidates for the above exploration. Particularly, a series of TM phthalocyanines (TMPcs), TM porphyrins (TMPs), and their derivatives have certain advantages over others. On the one hand, these molecular species are of extraordinary structural simplicity, chemical and thermal stability, making them widely used in kinds of single-molecule experiments [18,19]. Moreover, due to the ample choices for the central transition metal as well as the diversity of the organic ligands bonded to the metal center, their functionality can be changed in a controlled way [20]. For instance, TMPcs or TMPs with various substitutional central metal atoms on different substrates have been extensively employed as model systems in many-body quantum physics and spin-dependent transport phenomena, such as Kondo effect [21,22], negative differential resistance [23,24], magnetoresistance [25,26], and spin-flip excitation [27,28]. The richness and complexity of these physical behaviors have also shown the possibility to engineer the spin and magnetic anisotropy at the molecular scale, which is a prerequisite for the realization of ultimately miniaturized magnetic storage units [29,30].

However, the development of spin-based devices still face some challenges although considerable progresses have been made in the past two decades [31–33]. Currently, the typical spin-based applications particularly require long spin lifetimes, i.e., spin-relaxation and spin-coherence time to realize the successful generation, manipulation, and detection of spin and charge degrees of freedom [34]. Meanwhile, the development of high-density magnetic storage and memory devices at room temperature is especially demanding due to the need for sufficient magnetic anisotropy that can resist external perturbations [35,36]. It should be noted that if the spin is

*xgli@szu.edu.cn

coupled with a metallic substrate, spin-flip scattering of the conduction electrons typically limits the spin-lifetime scales drastically, and the possible Kondo effect, which is attributed to the screening of a localized magnetic moment by forming a correlated electron system with the surrounding conduction electrons, partially or completely quenches the magnetism of the system [37–39]. Therefore the operations of writing and reading the individual spin can not be realized effectively. To overcome these disadvantages, spins should be electronically decoupled from conduction electrons of the substrate, so that the corresponding spin-lifetimes can be elongated and the magnetic moment bearing orbitals are protected against external perturbations [35]. Considerable efforts have been devoted toward this direction by the use of different interlayers including insulating films and two-dimensional (2D) materials [40–42], additional TMPc molecular monolayer [27,43], rare-earth element [44,45], and different substrates including superconducting, semiconducting or heavy metallic substrates [35,46,47], etc.

Among all the above feasible approaches, 2D materials including graphene, hexagonal boron nitride (hBN), and transition metal dichalcogenides have attracted enormous interest due to their intriguing mechanical, optical and electronic properties, making them attractive candidates for various optoelectronic and electronic applications [48–50]. In particular, extensive theoretical and experimental investigations have revealed that epitaxial graphene and hBN are suitable to decouple the molecules from the underlying metal substrates by virtue of their chemical inertness and low density of states around the Fermi level. Recent studies have shown that certain hybrid molecule-metal interfaces involving 2D materials can serve an ideal platform for creating new spin effects, providing a representative route towards the realization of nanoscale architectures with robust magnetic and spintronic properties [42,51–53]. For example, sizable antiferromagnetic (AFM) or ferromagnetic (FM) indirect magnetic exchange interactions have been reported when a graphene interlayer was introduced between TMPc and ferromagnetic Co or Ni substrates [54–61]. Recently, Xu *et al.* have predicted that the tunneling barriers at the interface in CoPc adsorbed on 2D layered VSe_2 substrate are spin-dependent [62]. Wang *et al.* have realized the ferroelectric control of single-molecule magnetism on 2D α-In_2Se_3 substrate [63].

Several studies have been conducted on various types of TMPc molecules deposited on both bare FM substrates [64–68] and metal-supported graphene [54–57]. However, there is a lack of comprehensive research [58,68] on the fundamental mechanism underlying the impact of a graphene interlayer on the geometric and electronic properties of adsorbed molecules, particularly the exchange interaction between organic molecules and ferromagnetic spinterfaces. This knowledge is vital for the optimization of devices that rely on these molecules.

In this study, we conduct a systematic investigation into the structural, electronic and magnetic characteristics of divalent first-row magnetic TMPcs (TM = Cr, Mn, Fe, Co and Cu) adsorbed on graphene deposited on Ni(111). We employ first-principles calculations to provide detailed insights into the adsorption energetics, geometries, electronic structures and magnetic properties of the composite system. Specifically, we focus on examining the magnetic interactions at hybrid metal-molecule interfaces both before and after the introduction of the graphene interlayer. Our findings are then compared to existing experimental and theoretical research in the field. Our study reveals the presence of graphene not only reduces the strength of the magnetic coupling across the molecule-substrate interfaces, but also reverses its sign; the magnetic coupling in the CoPc/Ni(111) composite transitions from FM to AFM when graphene is inserted as an interlayer. These significant differences are attribute to the varied influences on the exchange interaction caused by the intermediary graphene layer. The inserted graphene layer may hinder the direct exchange interaction arising from the overlap between the out-of-plane d orbitals of the TM ion in TMPc and the Ni(111) surface, while the indirect superexchange interaction facilitated by the nitrogen atoms of the organic ligands is only reduced. This finding underscores the potential of utilizing graphene as a means to manipulate the magnetic characteristics of metal-molecule interfaces, a crucial aspect in the advancement of spintronic devices with enhanced performance capabilities.

The remainder of this paper is organized as follows. In Sec. II, the methodology and model employed for the theoretical investigation are introduced. Calculation results and the related theoretical analysis are presented in Sec. III. Concluding remarks are finally given in Sec. IV.

II. METHODOLOGY AND MODEL

A. Structural model of TMPc/Ni(111) and TMPc/Gr/Ni(111) composites

Figure 1(a) depicts the planar TMPc molecule, which contains a TM atom at its center and eight N neighbors: four pyridinic nitrogens and four pyrrolic nitrogens coordinated to the metal core. Ligand field theory indicates the magnetic moments of free TMPc molecules (TM= Cr, Mn, Fe, Co, Ni, Cu, and Zn) are 4, 3, 2, 1, 0, 1, and 0 μ_B, respectively [69–71]. Only these TMPc molecules with nonzero moments are of our interest, i.e., TM= Cr, Mn, Fe, Co, and Cu.

The Ni-supported graphene composited substrate, denoted as Gr/Ni(111) hereafter, is built by depositing a $\begin{bmatrix} 8 & 0 \\ 5 & 10 \end{bmatrix}$ supercell of graphene on a $\begin{bmatrix} 8 & 0 \\ 5 & 10 \end{bmatrix}$ supercell of Ni(111) surface. Here, the lattice constants of graphene and Ni are $a_{Gr} = 2.46$ Å and $a_{Ni} = 3.52$ Å [72], respectively. Hence the lattice mismatch of the constructed structure is calculated to be about 1.16%, justifying our theoretical considerations of commensurate geometries. Concerning the arrangement of the Gr/Ni(111) heterostructure, we restrict our discussion to the case of a graphene layer stacked on Ni(111) in the energetically favorable top-fcc geometry [72–75], where one C atom is adsorbed on top of a Ni atom and the other on an fcc hollow site of the Ni(111) surface.

When one TMPc molecule is directly adsorbed on the Ni(111) surface, there are four typical adsorption sites, namely top, hcp-hollow, fcc-hollow, and bridge [76]. Concerning the angle between the lobe of a TMPc molecule and the crystalline direction of the substrate gives more complicated conformations [77], and cannot be carried out in a large-scale systematic study as the one proposed here, we

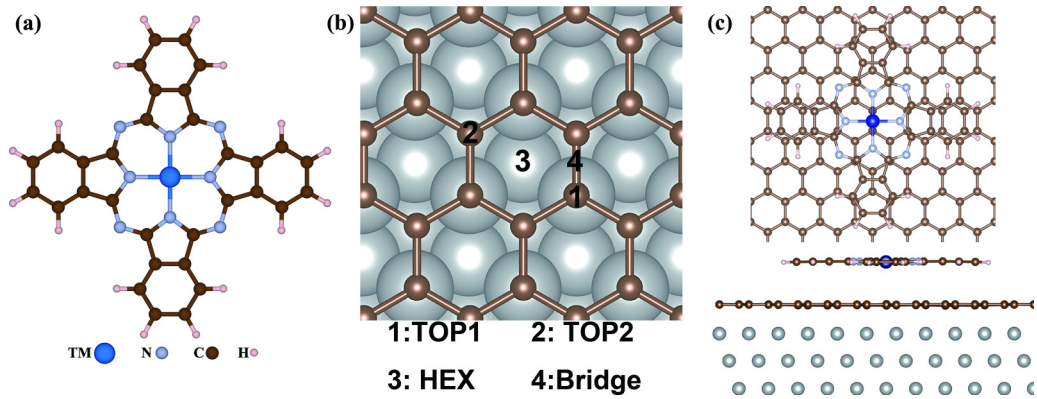

FIG. 1. (a) The chemical structure of a TMPc molecule. (b) Typical adsorption sites for single TMPc molecule on Gr/Ni(111). The labels 1, 2, 3, and 4 represent four high-symmetry positions within graphene, i.e., TOP1, TOP2, HEX, and Bridge, corresponding to the TM ion of the TMPc molecule located above two inequivalent C atoms, the hexagon center and above the center of a C–C bond, respectively. The graphene layer has top-fcc stacking with respect to the Ni(111) surface. (c) Top and side views of TMPc/Gr/Ni(111) with the bridge adsorption conformation. The Ni(111) substrate is omitted for a clear comparison in the upper figure.

consider only such four adsorption conformations for each TMPc in the present calculations.

Then we inspect four possible adsorption sites of TMPcs on Gr/Ni(111), denoted as TMPc/Gr/Ni(111) hereafter, by symmetry, sketched in Fig. 1(b): two sites on top of two inequivalent C atoms of graphene, i.e., "TOP1" where the C atom below the TM is on a Ni(111) top site and "TOP2" where this C atom is on the fcc-hollow site. The other two sites are the sixfold "HEX" and a "Bridge" between two C atoms. Such a setup consists of four layers of Ni(111) atoms with a monolayer graphene on one side (19.912 Å × 21.555 Å), which has a vacuum region of about 21 Å to reduce the slab's replica interaction along the z direction. The total number of atoms per cell amounts to 537 (320 Ni, 160 C, and 57 of the TMPc molecule).

B. Density functional theory calculations

Spin-polarized density functional theory (DFT) calculations have been performed using the projector augmented wave (PAW) method as implemented in the VASP code [78,79]. A cutoff energy of 400 eV for the plane wave basis is adopted. The Perdew–Burke–Ernzerhof (PBE) [80] version of generalized gradient approximation (GGA) for the exchange-correlation functional is used in combination with the DFT-D3BJ van der Waals (vdW) dispersion correction [81,82], which is suitable for the Ni-graphene interface [72]. Inclusion of vdW interactions in this approximation together with the GGA-PBE functional has been found to be a successful approach to describe interactions in similar graphene/substrate systems [72,83–85]. The localized character of the 3d orbitals is taken into account by the GGA $+U$ approach [86]. The effective $U_{\text{eff}} = U - J$ value has been chosen to be 3 eV. These values have been used in previous studies on similar systems [70,87,88].

Accurate determination of the magnetic exchange coupling across molecule-substrate spinterfaces is rather challenging based on the conventional DFT or quantum chemistry methods. It is known that the conventional DFT method can not adequately account for the multiplet structures displayed by TMPc molecules, such as FePc and MnPc [89–91]. Although the deficiencies of the DFT in accurately describing strongly correlated systems can be partially mitigated by incorporating a local Hubbard-like interaction [92,93], it is well-established that DFT $+ U$ calculations are prone to spurious convergence towards metastable states [94–97]. Additionally, it tends to overestimate the values of magnetic exchange coupling when compared to experimental observations. These apparent discrepancy is largely attributed to the fact that the symmetry of the charge (spin) densities is not sufficient to distinguish among different multiplets since all the multiplets generate densities of the same symmetry [89]. For instance, the Fe ion located at the FePc molecular center can give rise to three distinct triplet states with similar energy levels: ${}^3E_g(d_{xy}^2 d_{z^2}^1 d_\pi^3)$, ${}^3B_{2g}(d_{xy}^1 d_{z^2}^1 d_\pi^4)$, and ${}^3A_{2g}(d_{xy}^2 d_{z^2}^2 d_\pi^2)$. Various DFT methodologies have resulted in varying selections of triplets for the ground state of FePc [98,99], which is a long-standing debate in literature [100,101]. On the other hand, high-level quantum chemistry methods, such as the multiconfigurational wave functions method can treat multiplets of TMPc molecules more reliably [102–104], but their applications are limited to isolated molecules because of the high computational cost if applied in molecule-substrate composite systems. In order to achieve a balance between accuracy and computational efficiency in the calculations pertaining to the TMPc/Ni(111) and TMPc/Gr/Ni(111) composites, we have employed the PBE $+ U +$ vdW approach. This approach has been extensively utilized in prior studies to examine the magnetic exchange couplings at interfaces involving the adsorption of TMPc molecules on magnetic metallic surfaces or composite Gr/metal substrates [58,59,87,88]. By employing this methodology, we expect to enhance the precision of the anticipated geometric and electronic characteristics of the adsorption systems [70,105].

Initially, the geometry of the Gr/Ni(111) substrate was optimized. Subsequently, in the structural relaxations of TMPc/Gr/Ni(111), the positions of the graphene and metal

TABLE I. Calculated relative total energies (eV) of five kinds of TMPc molecules (TM=Cr, Mn, Fe, Co, Cu) adsorbed on different high-symmetry positions of Ni(111) and Gr/Ni(111) substrates. FM (AFM) refers to parallel (antiparallel) alignment of the TM spin moment of TMPc with respect to the Ni magnetization. The energy for the most stable position is set to zero (highlighted in bold font). "–" means the absence of a FM solution for the TOP1 configuration of CrPc/Gr/Ni(111).

	TOP		HCP		FCC		Bridge	
TMPc/Ni(111)	FM	AFM	FM	AFM	FM	AFM	FM	AFM
CrPc	1.779	1.808	0.339	0.393	0.390	0.403	**0**	0.066
MnPc	1.658	1.794	0.379	0.443	1.441	1.487	**0**	0.138
FePc	1.644	1.785	0.375	0.464	0.447	0.528	**0**	0.035
CoPc	1.752	1.826	0.427	0.433	0.461	0.498	**0**	0.013
CuPc	2.384	2.387	0.131	0.152	0.240	0.258	**0**	0.016
	TOP1		TOP2		HEX		Bridge	
TMPc/Gr/Ni(111)	FM	AFM	FM	AFM	FM	AFM	FM	AFM
CrPc	–	0.033	0.039	0.076	0.054	0.089	**0**	0.038
MnPc	**0**	0.071	0.036	0.078	0.061	0.131	0.025	0.081
FePc	**0**	0.016	0.029	0.056	0.060	0.091	0.047	0.086
CoPc	0.014	0.006	0.037	0.060	0.088	0.085	0.002	**0**
CuPc	0.035	0.051	0.051	0.053	0.088	0.098	**0**	0.004

layers were held constant based on the previously optimized geometry, while only the TMPc molecule underwent full relaxation. This setup has been tested and verified in literature [106]. For the TMPc/Ni(111), all atoms except for the bottom three Ni layers are fully relaxed. The convergence criterion for the total energy and the net force on every atom is set to 1×10^{-5} eV and 0.02 eV/Å, respectively. Because of the large size of the unit cell, structural optimizations adopt a Γ-centered k mesh only. In all calculations, a Gaussian smearing with a broadening of 0.05 eV is applied.

III. RESULTS AND DISCUSSION

A. Electronic structure and magnetic ground state

Table I summarizes the relative total energies of five kinds of TMPc molecules adsorbed on different high-symmetry positions of Ni(111) and Gr/Ni(111) substrates, with the total energy for the most favorite site set as the reference. Regarding the stability of the TMPc molecule directly adsorbed on Ni(111), the lowest energy from the geometry optimization has been obtained for the bridge position, i.e., on the bond between two surface Ni atoms, which is in agreement with previous calculations and experiments for TMPc on magnetic Co substrates [65,107,108]. After the graphene interlayer is inserted, CrPc, CoPc, and CuPc molecules favor the bridge position of graphene, meaning that the TM center of the molecule is positioned right on top of the bond between two graphene C atoms, while MnPc and FePc favor the top site, i.e., the TM center of the molecule is positioned right on top of a C atom of graphene [Fig. 1(b)]. This situation is in contrast to the cases of single TM atoms on Gr/Ni(111), where the bridge position is not stable and upon relaxation falls back to one of the other sites [75,109]. Generally, molecules adsorb on graphene mainly by vdW interactions [83,84,110]. Nevertheless, note that the difference in energies between different conformations of TMPc/Gr/Ni(111) is quite small; for instance, for CoPc, the energy difference between the "TOP1" and the "Bridge" adsorption sites is ∼6 meV, the latter site being favored, indicating that it is easy to move TMPc on the surface of graphene in a practical scenario. Such phenomenon is also found in TMPc adsorbed on inert surfaces such as Au(111) and Cu(111) [76,111]. Compared to TMPc directly adsorbed on Ni(111)—a more reactive metal surface, the order of magnitude in the energy difference between different conformations can reach to several eV, which also indicates the adsorption of TMPc on Ni(111) is much stable than that on Gr/Ni(111). In other words, the TMPc molecules are deemed to be chemisorbed on the Ni(111) surface, while physisorbed onto Gr/Ni(111). The chemisorption interactions at the interface in the former case can lead to the formation of chemical bonds between the molecular adsorbates and the substrate; see Figs. 2(e) and 4(e). Obviously, the strong interactions of TMPc with the underlying Ni substrate can be hindered by the insertion of the graphene interlayer. Our calculation results also support the conclusions of spectroscopy experiments on the same systems [112].

To make the picture of the substrate-induced effects more quantitative, we firstly examine the molecular geometry via (i) the average distance between the TMPc molecule and the substrate D_{m-s} is defined as the average height of the molecule minus the average height of the substrate. Here, D_{m-s} in TMPc/Gr/Ni(111) includes two parts D_{m-G} and D_{G-s}, which stand for the distance between the TMPc molecule and the graphene and the distance between the graphene and the top Ni layer, respectively; (ii) the vertical displacement of the TM center of TMPc against the ligand D_{c-l} in the molecule is defined as the height of the TM ion minus the height of the ligand, which stands for the degree of distortion from free-molecular planarity. Then the total magnetic moments of TMPc including the contribution from the TM atom are also summarized. The structural and magnetic properties of TMPc/Ni(111) and TMPc/Gr/Ni(111) are obtained from

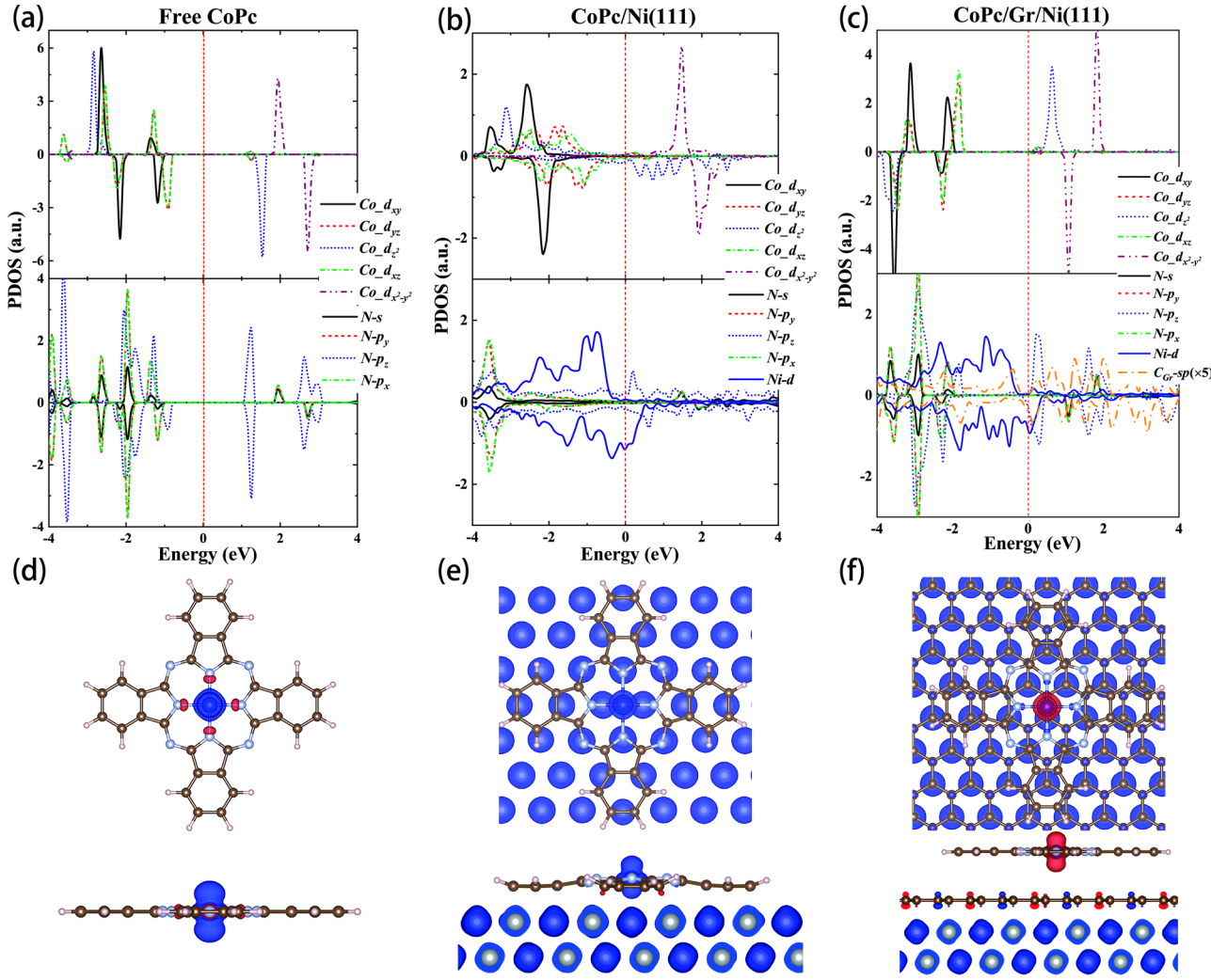

FIG. 2. The three panels (left to right) show the d-projected DOS of Co and sp-projected DOS of the N atoms in the (a) free CoPc, (b) the Bridge absorption configuration of CoPc/Ni(111), and (c) the Bridge absorption configuration of CoPc/Gr/Ni(111). We also show the out-of-plane d-projected DOS ($d_{z^2} + d_\pi$) of the Ni atom in topmost layer in (b) and (c), and the sp-projected DOS on the two different (by symmetry) C atoms of graphene in (c). The red vertical dash lines indicate the Fermi energy E_F that is set to zero. (d)–(f): top and side views of the system's spin density distributions. Blue (red) denotes positive (negative) spin density. The isosurface level for the spin density is 0.005 Bohr^{-3}. The spin densities are analyzed by VASPKIT [114] and rendered by VESTA [115].

the lowest energy configuration presented in Table I. Here, the reference for comparison is the D_{c-l} value in the free TMPc molecules. These properties are listed in Table II. When TMPc is deposited directly on the Ni(111) surface, the average molecule-substrate distance D_{m-s} is ∼2.2 Å for all five TMPc molecules, in agreement with reports on

TABLE II. The average distance (D_{m-s}) between the TMPc molecule and the substrate, the vertical displacement (D_{c-l}) of the TM center against the ligand and the total TMPc magnetic moment (M_{mol}) along with the contribution of the TM ion (M_{ion}) in the optimized free molecules, TMPc/Ni(111) and TMPc/Gr/Ni(111) composites (lengths in Å, magnetic moment in μ_B). These data are extracted from the lowest energy configuration of TMPc/Ni(111) and TMPc/Gr/Ni(111) in Table I. For comparison, D_{c-l} in the free TMPc molecules are set as reference.

	Free			On Ni(111)				On Gr/Ni(111)			
TMPc	D_{c-l}	M_{mol}	M_{ion}	D_{m-s}	D_{c-l}	M_{mol}	M_{ion}	D_{m-G}	D_{c-l}	M_{mol}	M_{ion}
CrPc	0	4.00	3.55	2.19	0.24	3.21	3.41	3.25	0.03	3.33	3.53
MnPc	0	3.00	3.42	2.23	0.17	4.23	4.21	3.24	0.00	2.81	3.47
FePc	0	2.00	2.15	2.19	0.18	2.01	1.91	3.25	0.00	1.71	2.01
CoPc	0	1.00	1.04	2.18	0.16	0.71	0.65	3.24	0.02	1.03	1.01
CuPc	0	1.00	0.59	2.17	0.16	0.44	0.71	3.26	0.00	0.85	0.59

similar systems [65,113]. Such short distance also indicates the chemisorption on the Ni(111) surface. In contrast, the molecule-graphene distance enlarges to ∼3.2 Å after the graphene interlayer inserted, meanwhile the graphene-metal distance D_{G-s} stays almost unchanged (2.1 Å). Obviously, such large molecule-substrate distance indicates the TMPc molecules are physisorbed onto Gr/Ni(111). Moreover, as can be found in Table II, the data D_{c-l} standing for the molecular distortion confirm the aforementioned presumptions: regarding some deviation from the molecular in-plane position occurs for the macrocyclic atoms, D_{c-l} increases to a considerable amount of 0.16–0.24, which indicates the planar molecular geometry of free molecule ($D_{c-l} = 0$) is distorted after depositing on Ni(111); see Fig. 2(e) for example illustration. While in the presence of graphene, the data D_{c-l} in TMPc/Gr/Ni(111) are almost zero, in agreement with our observation of a mostly unperturbed molecule; see Fig. 2(f). Meanwhile, a similar behavior can be found from the magnetism data M_{mol} and M_{ion} in Table II, where the magnetic moments of the TMPc molecules undergo a considerable change when directly adsorbed on the Ni(111) surface but recover to their free state values in the presence of a graphene interlayer.

To achieve further insights into the chemisorption and physisorption behaviors on different substrates, we then calculated the ground-state electronic structure including the spin density distribution and spin-polarized projected densities of states (PDOS) in free, TMPc/Ni(111) and TMPc/Gr/Ni(111) composites. Here, we take the case of CoPc for an example. As depicted in the lower panels of Fig. 2, the spin density distribution of the molecule in three cases mainly concentrates at the Co center spreads to the near four pyrrolic N atoms of the Pc ligands, while the latter possesses a very small but opposite direction with respect to the Co magnetism. As shown in Fig. 2(a) for free CoPc, the spin-polarized d_{z^2} orbital contributes significantly to the total magnetic moment 1.0 μ_B along with the local electronic configuration of $(d_{xy})^2(d_\pi)^4(d_{z^2})^1$. For comparison, the PDOS distributions of the Co-d and N-p orbitals of CoPc are changed dramatically after deposited on the Ni surface. Firstly, while the Co-d_π and N-p_x (p_y) orbitals are almost degenerate in the free molecule, they exhibit a small offset on Ni(111). Obviously, this indicates the planarity of the free molecule is distorted; see Figs. 2(d) and 2(e). In particular, compared to the free CoPc molecule whereas the PDOS distribution of all the orbitals appears a collection of isolated peaks [Fig. 2(a)], the shape of the out-of-plane orbitals including Co-d_π, Co-d_{z^2} and N-p_z are broadened over several electronvolts below E_F (the in-plane Co-d_{xy} and $d_{x^2-y^2}$ orbitals are also broadened, but the degree is much smaller), resulting in a reduced magnetic moment of 0.7 μ_B of CoPc. These observations demonstrate the presence of significant interactions between the Co center and the Ni substrate, as well as between the molecular macrocycle and Ni. Figure 2(e) also depicts that the chemical bonding of the molecule to the surface is between Ni surface atoms and N atoms of CoPc.

When a graphene interlayer is inserted between CoPc and Ni, the computed electronic structure of CoPc closely resembles that of the isolated molecule, with the exception that the spin polarization direction is reversed and the PDOS distributions are shifted entirely to the left; see Figs. 2(a) and 2(c). This can be well understood from the analyses of geometry of CoPc/Gr/Ni(111). As listed in Table II, the optimized distance D_{m-G} between CoPc and graphene is 3.24 Å, meanwhile graphene is located above 2.14 Å from Ni(111), and hence CoPc is placed 5.38 Å above Ni(111). Such large distance implies the fact that the vdW interaction dominates in the system. For the same reason, the ideal planar molecular geometry of CoPc is almost retained [the tiny $D_{c-l} = 0.02$ also confirms the conclusion]. Our calculations thus depict the CoPc molecule as physisorbed onto Gr/Ni(111) with the electronic property being close to that of free-standing. Accordingly, the above results demonstrate explicitly that the TMPc molecule is chemisorbed on the bare Ni substrate, losing its previous electronic and even geometric footprints. However, the insertion of the graphene interlayer tends to prevent strong molecule-substrate interactions, allowing the molecule to recover to its free state.

TABLE III. Calculated the exchange energy E_{ex} (units in meV) data for the TMPc/Ni(111) and TMPc/Gr/Ni(111) composites.

System	CrPc	MnPc	FePc	CoPc	CuPc
On Ni(111)	65.5	138.1	34.6	13.3	15.6
On Gr/Ni(111)	38.3	71.2	15.7	−1.5	4.2

Previous studies for similar TMPc deposited on nonmagnetic metal-supported graphene reported the molecular properties are preserved in the TMPc/Gr/Au(111) composites [84]. Obviously, the magnetism of the metallic substrate has a trivial effect on the interaction between the TMPc molecule and the composited substrate. The graphene has shown the ability to decouple adsorbed molecules from underlying substrate thereby preserving the symmetry of molecular orbitals responsible for magnetic behavior of molecules [42,112]. Similar procedures also could be established for the other TMPc/Gr/Ni(111) (TM=Cr, Mn, Fe and Cu) composites; see Fig. 4 and Figs. S1–S3 in Ref. [116].

In particular, our DFT results reveal that the sign and magnitude of the magnetic coupling between the spins of TMPc and the magnetic Ni substrate can be mediated by the insertion of graphene. Here, concerning the magnetic properties of ground states we present the exchange energy $E_{ex} = E_{tot}^{AFM} - E_{tot}^{FM}$ defined as the energy difference between the most stable AFM and FM solutions, with the 3d spin moment of TMPc coupled antiparallel or parallel to the Ni magnetization, respectively [116]. Positive (negative) values indicate that FM (AFM) coupling is favored between the TMPc and Ni substrate spins. As summarized in Table III, all TMPc molecules prefer the FM coupling when directly adsorbed on the bare Ni substrate, in agreement with previous reports on related systems [120], while this FM coupling is retained but its strength is weakened in the presence of graphene interlayer except for CoPc, where a magnetic transition from FM to AFM is achieved.

Previous DFT investigations have revealed that the calculated values of the magnetic exchange couplings between TMPc molecules and substrates generally lie within the range of several tens of meV [58,87,88]. As listed in Table III,

our DFT calculations indicate that the FePc molecule exhibits a preferred FM coupling with the Ni substrate with a value of 34.6 meV. However, the presence of a graphene layer significantly reduces this coupling to 15.7 meV. Notably, the direction and strength of these couplings align well with the findings of previous study [58]. We also note that for the case of FePc adsorbed on a Co(001) surface, the coupling value is 229 meV [87]. In contrast, the experimental measurements give the values of 1.2 and 0.5 meV for FePc on the Ni substrate and Gr/Ni(111), respectively [58]. Obviously, the DFT method tends to overestimate the coupling values when compared to experimental findings, which can be attributed, at least in part, to the lack of electronic correlation effects inherent in mean-field electronic structure calculations [58]. This observation has been noted in previous studies of a similar nature [55,59]. However, it is worth noting that our study has successfully captured the overall trend of the interaction on both the Ni substrate and the Gr/Ni(111) composite substrate, which aligns with empirical experiments.

B. Mechanism of magnetic coupling

As summarized in Table III, our DFT results reveal that magnetic couplings at organic molecular/ferromagnet interfaces can be modified by inserting a single layer of graphene. These findings provide interesting cases compared to those known from earlier studies of similar systems. The so-far observed coupling between the metal-organic species and the FM substrates in literature can be classified as follows:

(i) direct FM exchange interaction [66,113];

(ii) indirect 90° FM exchange interaction [64,67,121,122];

(iii) indirect AFM exchange interaction via organic ligands, oxygen or graphene [55,68,88,123–125];

(iv) oscillatory Ruderman-Kittel-Kasuya-Yosida (RKKY) exchange interaction [126].

Generally, when metal-porphyrins and phthalocyanines are directly deposited on FM metal films [64–68,113,121,123,127], the magnetic moment of the metal centers can efficiently interact with substrate electronic states via direct exchange or indirect superexchange paths, or both, considering the planar structure of such molecules and close proximity of the metal ions to the substrate. The direct exchange path mainly occurs between the out-of-plane orbitals of the TM center and metallic substrates [66,113], while the indirect superexchange path can be triggered by the aid of the nitrogen atoms of the organic ligands [64,67,68,122,125]. Two of the most important factors which control the sign and strength of such magnetic couplings are the degree of orbital overlap and the charge transfer, which depend crucially on the unpaired electrons and the vacant orbitals on the metal centers [128]. As reported for all planar complexes deposited on FM metal surfaces to date, the interaction between the magnetic moment of the molecules and that of metal substrates has been found to be FM [120]. However, it has been noted that when oxygen (O) or graphene is introduced between the molecules and substrates, the coupling has been found to be AFM [55,88,123]. Following the introduction of a graphene sheet between the TMPc molecule and the magnetic substrate, the direct exchange interaction, characterized by its limited range, is impeded by the presence of the graphene layer. Instead, a more complex superexchange mechanism is considered to enable a magnetic interaction over a substantial distance. Note that the π orbitals of graphene become magnetically polarized as a result of hybridization with the Ni-d states of the substrate [129]. Consequently, these polarized π orbitals of graphene are able to engage in such superexchange interactions across the TMPc-Ni(111) interface [55,59,60]. For instance, a 180° superexchange interaction involving the out-of-plane molecular orbitals (d_{z^2} and d_π) is responsible for the graphene-mediated AFM coupling in the TMPc/Gr/Co composites (TM=Mn and Fe), while a 90° FM superexchange path is triggered, with the magnetic coupling being transferred through the N-p orbitals, strongly hybridized the in-plane molecular orbitals ($d_{x^2-y^2}$) in the CuPc/Gr/Co composite [59,60].

Our DFT calculations give the ground-state electronic configuration of the TM ion in the free TMPc molecule as $(d_{xy})^1(d_{z^2})^1(d_\pi)^2$ ($S = 2$ for CrPc), $(d_{xy})^1(d_{z^2})^1(d_\pi)^3$ ($S = 3/2$ for MnPc), $(d_{xy})^1(d_{z^2})^1(d_\pi)^4$ ($S = 1$ for FePc), $(d_{xy})^2(d_{z^2})^1(d_\pi)^4$ ($S = 1/2$ for CoPc) and $(d_{xy})^2(d_{z^2})^2(d_\pi)^4(d_{x^2-y^2})^1$ ($S = 1/2$ for CuPc), respectively; see Figs. 2, 4, and Figs. S1–S3 in Ref. [116]. Similar ground states have been reported in previous DFT studies for free TMPc molecules [84,85]. Regarding the fact that the free CoPc molecule possesses a half-filled d_{z^2} orbital with the out-of-plane symmetry, and CuPc has a half-filled $d_{x^2-y^2}$ orbital with the in-plane symmetry, we can thus view these two TMPc molecules as simplified models to understand how the magnetic interactions between the molecules and the substrates occur.

We firstly focus on the case of CoPc on Ni(111). As compared to the free molecule, the spin polarization of the adsorbed CoPc molecule are enhanced. As depicted in Fig. 2(b), it is apparent that the CoPc molecule displays an intrinsic disparity between its spin-up and spin-down states within a defined energy range. Hence the molecule possesses a magnetic moment that is mainly localized on the Co ion and distributed little in the porphyrin ligands, as illustrated in Fig. 2(e). We can conclude the ground-state electronic configuration of the Co ion in the CoPc/Ni(111) composite is approximately as $(d_{xy})^2(d_{z^2})^1(d_\pi)^4$ with a spin $S = 1/2$. The overall magnetic moment of the molecule primarily arises from the Co-d_{z^2} orbital. On the other hand, for the preferred bridge site of CoPc on Ni(111), the distance between the Co ion and the Ni(111) surface is 2.34 Å, which is in close proximity to the Ni-Ni bond length of 2.49 Å. Additionally, the average distance between CoPc and Ni(111) is measured to be 2.18 Å, with a surface distortion of only 0.12 Å or lower occurring; see Table II and Fig. 2(e). These findings suggest that the magnetic coupling between CoPc and Ni(111) can occur either by a direct exchange interaction with the out-of-plane orbitals of the Ni substrate or via an indirect exchange interaction through the nitrogen orbitals; see Fig. 3(a) for illustration. The former is attributed to the considerable overlap between the d_{z^2} orbital of Co and out-of-planes orbitals of Ni, which would be accompanied by FM coupling [65,68], leading to the notable broadening of the d_{z^2} orbital of Co. The latter indicates an indirect superexchange interaction between the d_π orbital of Co and out-of-planes orbitals of Ni through

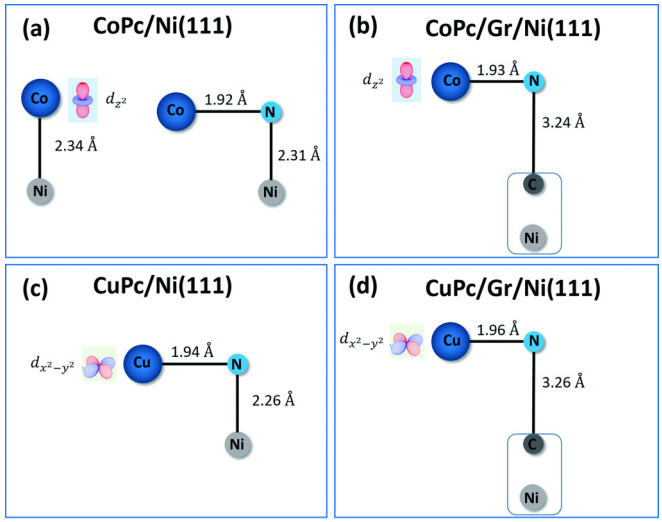

FIG. 3. The two panels show schematic diagrams of the interaction mechanism in TMPc/Ni(111) and TMPc/Gr/Ni(111) composites (TM=Co, Cu). (a) The half-filled out-of-plane d_{z^2} orbital of the Co ion can directly interact with the out-of-plane orbitals of the Ni substrate, or indirectly with the out-of-plane orbitals of the Ni substrate via the N-p orbital of the organic ligands. (b) The half-filled out-of-plane d_{z^2} orbital of the Co ion indirectly interacts with the comparable Gr/Ni(111) substrate by the aid of the N atoms of the organic ligands. (c) The half-filled in-plane $d_{x^2-y^2}$ orbital of the Cu ion indirectly interacts with the out-of-plane orbitals of the Ni substrate via the N-p orbitals of the organic ligands. (d) The half-filled in-plane $d_{x^2-y^2}$ orbital of the Cu ion participates in the indirect superexchange interaction with the comparable Gr/Ni(111) substrate by the aid of the N-p orbitals of the organic ligands. Inset images in (a)–(d) show the involved magnetic TM-d orbitals. Box in (b) and (d) denotes the comparable metallic substrate consisting of Gr/Ni(111).

the N-p_z orbitals [68]. Since the latter superexchange is a long-range interaction occurring over a significant distance and the involved d_π orbital of Co are full-filled, this indirect interaction would be much weaker that the direct one. We thus attribute the dominant coupling between Co and Ni to a direct coupling, as evidenced in similar systems [65,113]. We also note that such indirect interaction could make a broadening of the Co-d_π orbitals in DOS occurs in Fig. 2(b). As a result, our calculations suggest the magnetic CoPc molecule prefers a direct FM coupling with the Ni(111) surface. The findings align with the previously documented observations regarding the behavior of CoPc on a Co surface [65].

When a graphene interlayer is inserted between the CoPc molecule and the Ni substrate, the PDOS distribution of CoPc closely resembles that of an isolated molecule, preserving the comparable electronic structure of the ground state, specifically $(d_{xy})^2(d_\pi)^4(d_{z^2})^1$; see Figs. 2(a), 2(c). The half-filled d_{z^2} orbital mainly determines the spin density distribution on the Co ion [Fig. 2(f)]. Considering the significant separation between the CoPc molecule and the graphene layer (3.24 Å) makes the overlap between the localized Co-d_{z^2} and graphene π orbitals negligible. However, there remains a slight overlap between the delocalized macrocyclic π orbital of CoPc and the graphene π orbital [55]. It is inferred that the direct interaction between CoPc and graphene is improbable, instead the molecule only engages indirectly with the spin polarization of Ni by the aid of the N atoms of ligands and graphene. In detail, the π orbitals of graphene are magnetically polarized due to hybridization with the Ni-d states of the substrate, and it hybridize weakly with the macrocyclic π orbitals, leading to a small positive spin density mainly on the N atoms [Fig. 2(f)]. The spin densities on the N atoms couple to the spins on the Co ion of the molecule, together with Pauli' s exclusion principle, force the Co-d_{z^2} electron to align its spin antiparallel to the spins of the N atoms. Consequently, the magnetic moment of CoPc is aligned by a weak AFM coupling to the Ni substrate underneath the graphene, in agreement with the conclusion by Avvisati *et al.* regarding similar molecules [59,60]. This coupling can be likened to an indirect superexchange interaction between the CoPc molecule and a comparable metallic substrate; see Fig. 3(b) for illustration. Here, graphene on Ni(111) can be regarded as such a comparable metallic substrate, as the laterally extended π states of graphene are demonstrated its metal-like electronic characteristics within the plane when graphene is deposited on Ni(111) [129]. Meanwhile, the strength of such superexchange interaction across the graphene layer as opposed to CoPc adsorbed directly on reactive ferromagnetic substrates is comparatively small. Indeed, the value $E_{\text{ex}} = -1.5$ meV for CoPc/Gr/Ni(111) is much smaller than that in CoPc/Ni(111); see Table III. Our results show that the magnetic coupling between CoPc and Gr/Ni(111) exhibits a sign and magnitude that aligns with the findings reported for a similar planar molecule, namely CoOEP on Gr/Ni(111) [55].

We then consider the case of CuPc on Ni(111). As depicted in Fig. 4(b), the distinct peaks observed in the d and p orbitals in an isolated CuPc molecule undergo considerable broadening upon adsorption. This broadening phenomenon can be attributed to the robust interaction between the CuPc molecule and the Ni substrate. The distribution of PDOS for CuPc reveals that the spin polarization of the adsorbed CoPc molecule is significantly enhanced, particularly for the macrocyclic portion of the molecule. However, within the energy range below the Fermi level, the number of spin-up and spin-down states for the d_π, d_{z^2}, and d_{xy} orbitals is nearly equal. The overall magnetic moment of the molecule primarily originates from the Cu-$d_{x^2-y^2}$ and N-p orbitals. Note that the Cu ion sits on a bridge position between two surface Ni atoms at a Cu-Ni distance of 2.32 Å, and the average molecule-substrate distance is approximately 2.17 Å (Table II). Considering the involved $d_{x^2-y^2}$ orbital is magnetically polarized with a dominant in-plane symmetry (we should note that here CuPc is different from the CoPc case which has the half-filled d_{z^2} orbital with out-of-plane symmetry), it can be inferred that the interaction between CuPc and Ni(111) primarily occurs through an indirect exchange interaction by the aid of the N atoms of the organic ligands. The direct interaction between the out-of-plane Cu orbitals (d_π and d_{z^2} are full-filled) and Ni is much weaker, and overshadowed by significant changes to the in-plane Cu-N orbitals ($d_{x^2-y^2}$ and p_x, p_y). In detail, the N-p_x orbital hybridizes with the Cu-$d_{x^2-y^2}$ orbital and a σ-type bond is formed between them, whereas the bonding to the Ni out-of-plane orbitals occurs via interaction of the N-p_z orbital in the macrocycle of CuPc, as can be recognized from

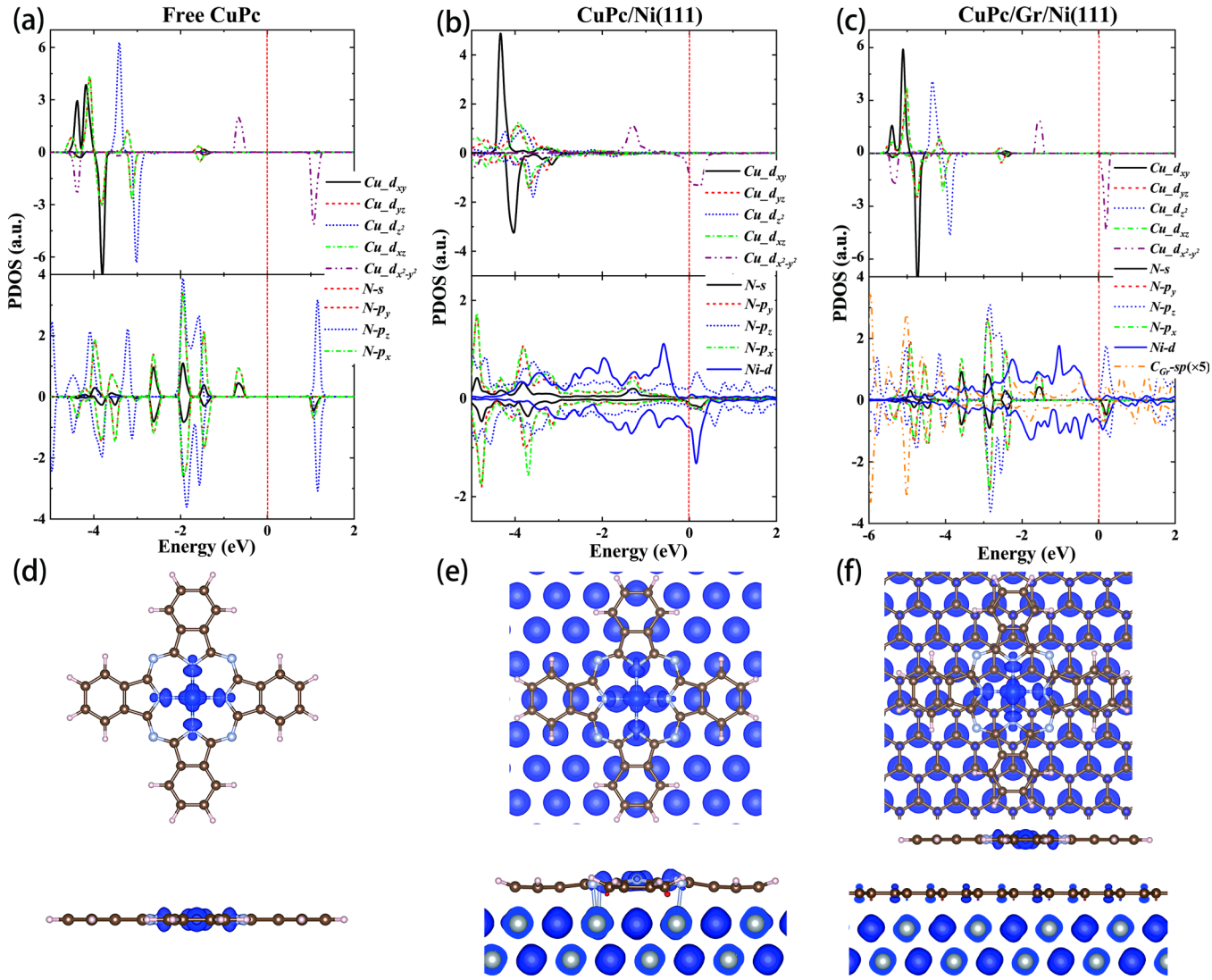

FIG. 4. The three panels (left to right) show the spin-polarized PDOS of the molecule in the (a) free CuPc, (b) the bridge configuration of CuPc/Ni(111), and (c) the bridge configuration of CuPc/Gr/Ni(111). (a)–(f) adopt the same convention as in Fig. 2.

the occurrence of peaks close in energy between −3 to −4 eV for the p states of N and d states of Ni; see Fig. 4(b). Due to the intra-atomic FM interaction between nitrogen orbitals, the $d_{x^2-y^2}$ orbital will experience a strong exchange interaction with the polarized N orbitals, resulting in a parallel alignment of magnetic moments of Cu and N atoms [Fig. 4(e)]. Here, the angles between the Ni surface atom, the N atom on top, and the Cu ion from CuPc are close to 90°, corresponds to a FM superexchange coupling according to the Goodenough-Kanamori rules [130]. As a result, the spin of CuPc is FM coupled to the Ni substrate, as evidenced by our DFT + U calculations; see Fig. 3(c) for illustration.

In the presence of graphene interlayer between the CuPc moleclue and the Ni substrate, the electronic configuration of the Cu ion in the CuPc/Gr/Ni(111) composite is analogous to that in the free case, which is $(d_{xy})^2(d_\pi)^4(d_{z^2})^2(d_{x^2-y^2})^1$ [Figs. 4(a) and 4(c)]. The substantial separation of 3.26 Å between the CuPc molecule and graphene suggests that the direct interaction between the molecule and substrate is improbable. Considering Gr/Ni(111) as a magnetic unit, it is plausible that the half-filled in-plane Cu-$d_{x^2-y^2}$ orbital may undergo an indirect superexchange interaction with the substrate facilitated by the pyrrolic N atoms. This scenario resembles the behavior observed in the CuPc/Ni(111) composite; see Figs. 3(c) and 3(d) for illustration. Accordingly, the magnetic moment of CuPc can be aligned by a FM coupling to the comparable metallic substrate by the aid of the N atoms of the organic ligands, in excellent agreement with the conclusion by Avvisati *et al.* regarding similar molecules [59,60]. It should be noted that the distance of 3.26 Å between the CuPc molecule and graphene is greater than the average distance of 2.17 Å between the molecule and Ni(111). Consequently, the FM coupling strength in CuPc/Gr/Ni(111) is significantly weaker than that in CuPc/Ni(111); see Table III.

Based on the above analysis to the cases of CoPc and CuPc, it is instructive to conclude the varied impacts on the exchange interaction caused by the intermediary graphene layer. The presence of the inserted graphene layer may hinder the direct exchange interaction across the molecule-substrate interfaces, e.g., for CoPc, while the indirect superexchange interaction

facilitated by the nitrogen atoms of the organic ligands is only reduced, e.g., for CuPc. Similar procedures also could be established to explain the variation of magnetic couplings for the cases of CrPc, MnPc, and FePc; see Ref. [116].

C. Discussion

Our calculations indicate that the adsorbed TMPc molecule retains a localized magnetic moment on both Ni(111) and Gr/Ni(111) substrates. In general, the interplay between local magnetic moments and their surrounding environment can lead to a variety of fascinating physical phenomena, including the Kondo effect and spin excitation. These phenomena have been observed in transport experiments that involve magnetic adsorbates on various types of hosts [21,22,126,131–140]. While the majority of experimental studies have primarily concentrated on the interaction between magnetic impurities and a nonmagnetic metallic host, there have been many theoretical and experimental investigations exploring the impact of ferromagnetic electrodes on the transport characteristics in the Kondo effect [131–134,136]. Additionally, theoretical predictions have suggested that magnetic impurities on monolayer graphene can exhibit the Kondo effect [141], experimental evidence of the Kondo effect has been observed specifically for Co on graphene on Ru(0001) substrate [142]. In the cases of magnetic TMPc molecules on graphene, the evidence of the Kondo effect is also rarely reported in relevant STM experiments [135,143].

In order to gain a deeper understanding of the underlying factors contributing to these phenomena, we will examine the necessary conditions for the manifestation of a Kondo resonance within the framework of the single impurity Anderson model (SIAM). The employment of this particular model is supported by the following observations: (i) The composite of TMPc/Gr/Ni(111) exhibits a localized spin magnetic moment on the TM center, and the SIAM effectively accounts for the screening of these local spin moments by itinerant electrons. (ii) The magnetism of the system is primarily influenced by spin-unpaired d orbitals, with minimal contribution from other orbitals. For example, the CoPc/Gr/Ni(111) composite is tentatively recognized as a spin-1/2 SIAM that can be used to investigate the potential Kondo effect. The associated Kondo temperature, denoted as T_K, can be expressed as follows [144]:

$$k_B T_K \simeq \sqrt{\frac{JU}{2}} \exp\left[-\frac{\pi(\epsilon+U)|\epsilon|}{2JU}\right]. \quad (1)$$

Here, J represents the effective coupling between the p_z orbitals of graphene and the magnetic d_{z^2} orbital of the Co ion. Additionally, U denotes the Coulomb repulsion, while ϵ represents the impurity orbital energy of the d_{z^2} orbital. The values of U and ϵ can be determined by analyzing the results obtained from DFT calculations [43,99]. The parameters for the CoPc/Gr/Ni(111) composite are determined to be (in units of eV) $\epsilon = -3.50$, $U = 5.76$, and $J = 0.11$. By utilizing Eq. (1), we calculate the Kondo temperature $T_K \sim 1.9 \times 10^{-5}$ K. However, this value is deemed too low to be detected under the present experimental conditions. In the case of other composites of TMPc/Gr/Ni(111), it is also improbable to detect the potential Kondo effect through spectroscopic properties. This is attributed to the electronic decoupling of the molecules from the metal substrate facilitated by the graphene monolayer. Consequently, the Kondo temperature becomes too low to be observable. Indeed, the detection of the spin excitation signal, rather than the Kondo effect, has been experimentally observed in composites consisting of TMPc/graphene/substrates [137,138].

As demonstrated by the above analysis, the introduction of graphene between TMPc and Ni(111) in experimental setups can be confirmed by observing the behavior of related signals, such as the Kondo resonance and spin excitation in the dI/dV spectra. Therefore it can be inferred that the TMPc/Ni(111) and TMPc/Gr/Ni(111) composites serve as exemplary systems for studying the concept of chemical manipulation of the Kondo effect and spin excitation at the nanoscale.

IV. CONCLUSION

In summary, our work demonstrates that graphene plays a vital role in mediating the exchange interactions between magnetic TMPc molecules and ferromagnetic Ni substrates. Through systematic analyzing the mechanisms of exchange interaction by structural models constructed from our DFT calculations, we find that the presence of the inserted graphene layer can hinder the direct exchange interaction arising from the overlap between the out-of-plane d orbitals of the TM ions in TMPc and the Ni(111) surface, while reduce the indirect superexchange interaction by the aid of the nitrogen atoms of the organic ligands. These effects not only affect the magnitude of the magnetic interaction between the spins of TMPc and the Ni substrate but also result in a reversal of its direction in the CoPc/Ni(111) composite. In the instance of CoPc, the initial FM coupling with Ni(111) can be transformed into an AFM interaction when a graphene interlayer is incorporated. Although the DFT + U method utilized in this study does not provide an exact determination of the coupling values at molecule-substrate interfaces, our calculations have successfully captured the overall trend of the interaction on both the Ni substrate and the Gr/Ni(111) composite substrate, achieving a balance between precision and computational efficiency. Ongoing research is focused on refining the calculation method for improved accuracy.

ACKNOWLEDGMENTS

This work was supported by the National Natural Science Foundation of China (Grants No. 12004255, No. 22309113, and No. 12274301). The computational resources are partly provided by the National Supercomputing Center in Guangzhou.

All authors declare that they have no conflicts of interest.

[1] L. Bogani and W. Wernsdorfer, Molecular spintronics using single-molecule magnets, Nat. Mater. **7**, 179 (2008).

[2] S. Sanvito, Molecular spintronics, Chem. Soc. Rev. **40**, 3336 (2011).

[3] S. Jiang, K. Goß, C. Cervetti, and L. Bogani, An introduction to molecular spintronics, Sci. China Chem. **55**, 867 (2012).

[4] W. Kuch and M. Bernien, Controlling the magnetism of adsorbed metal-organic molecules, J. Phys.: Condens. Matter **29**, 023001 (2017).

[5] L. Guo, X. Gu, X. Zhu, and X. Sun, Recent advances in molecular spintronics: Multifunctional spintronic devices, Adv. Mater. **31**, 1805355 (2019).

[6] H. Chen and J. Fraser Stoddart, From molecular to supramolecular electronics, Nat. Rev. Mater. **6**, 804 (2021).

[7] N. Ballav, C. Wäckerlin, D. Siewert, P. M. Oppeneer, and T. A. Jung, Emergence of on-surface magnetochemistry, J. Phys. Chem. Lett. **4**, 2303 (2013).

[8] K. V. Raman, Interface-assisted molecular spintronics, Appl. Phys. Rev. **1**, 031101 (2014).

[9] M. Cinchetti, V. A. Dediu, and L. E. Hueso, Activating the molecular spinterface, Nat. Mater. **16**, 507 (2017).

[10] M. Sun and W. Mi, Progress in organic molecular/ferromagnet spinterfaces: towards molecular spintronics, J. Mater. Chem. C **6**, 6619 (2018).

[11] A. Kumar, Advances in tetrapyrrole complexes spin interfaces, Mater. Today: Proc. **37**, 2858 (2021).

[12] E. Pandey, P. Sharangi, A. Sahoo, S. P. Mahanta, S. Mallik, and S. Bedanta, A Perspective on multifunctional ferromagnet/organic molecule spinterface, Appl. Phys. Lett. **123**, 040501 (2023).

[13] M. Mannini, F. Pineider, P. Sainctavit, C. Danieli, E. Otero, C. Sciancalepore, A. M. Talarico, M.-A. Arrio, A. Cornia, D. Gatteschi, and R. Sessoli, Magnetic memory of a single-molecule quantum magnet wired to a gold surface, Nat. Mater. **8**, 194 (2009).

[14] K. V. Raman, A. M. Kamerbeek, A. Mukherjee, N. Atodiresei, T. K. Sen, P. Lazić, V. Caciuc, R. Michel, D. Stalke, S. K. Mandal, S. Blügel, M. Münzenberg, and J. S. Moodera, Interface-engineered templates for molecular spin memory devices, Nature (London) **493**, 509 (2013).

[15] T. Miyamachi, M. Gruber, V. Davesne, M. Bowen, S. Boukari, L. Joly, F. Scheurer, G. Rogez, T. K. Yamada, P. Ohresser, E. Beaurepaire, and W. Wulfhekel, Robust spin crossover and memristance across a single molecule, Nat. Commun. **3**, 938 (2012).

[16] M. N. Leuenberger and D. Loss, Quantum computing in molecular magnets, Nature (London) **410**, 789 (2001).

[17] J. Lehmann, A. Gaita-Ariño, E. Coronado, and D. Loss, Quantum computing with molecular spin systems, J. Mater. Chem. **19**, 1672 (2009).

[18] T. Niu and A. Li, Exploring single molecules by scanning probe microscopy: Porphyrin and phthalocyanine, J. Phys. Chem. Lett. **4**, 4095 (2013).

[19] J. M. Gottfried, Surface chemistry of porphyrins and phthalocyanines, Surf. Sci. Rep. **70**, 259 (2015).

[20] W. Auwärter, D. Écija, F. Klappenberger, and J. V. Barth, Porphyrins at interfaces, Nat. Chem. **7**, 105 (2015).

[21] A. Zhao, Q. Li, L. Chen, H. Xiang, W. Wang, S. Pan, B. Wang, X. Xiao, J. Yang, J. G. Hou, and Q. Zhu, Controlling the Kondo effect of an adsorbed magnetic ion through its chemical bonding, Science **309**, 1542 (2005).

[22] L. Gao, W. Ji, Y. B. Hu, Z. H. Cheng, Z. T. Deng, Q. Liu, N. Jiang, X. Lin, W. Guo, S. X. Du, W. A. Hofer, X. C. Xie, and H.-J. Gao, Site-specific kondo effect at ambient temperatures in iron-based molecules, Phys. Rev. Lett. **99**, 106402 (2007).

[23] L. Chen, Z. Hu, A. Zhao, B. Wang, Y. Luo, J. Yang, and J. G. Hou, Mechanism for negative differential resistance in molecular electronic devices: Local orbital symmetry matching, Phys. Rev. Lett. **99**, 146803 (2007).

[24] X. W. Tu, G. R. Mikaelian, and W. Ho, Controlling single-molecule negative differential resistance in a double-barrier tunnel junction, Phys. Rev. Lett. **100**, 126807 (2008).

[25] B. Warner, F. El Hallak, H. Prüser, J. Sharp, M. Persson, A. J. Fisher, and C. F. Hirjibehedin, Tunable magnetoresistance in an asymmetrically coupled single-molecule junction, Nat. Nanotechnol. **10**, 259 (2015).

[26] K. Yang, H. Chen, T. Pope, Y. Hu, L. Liu, D. Wang, L. Tao, W. Xiao, X. Fei, Y.-y. Zhang, H.-g. Luo, S. Du, T. Xiang, W. A. Hofer, and H.-j. Gao, Tunable giant magnetoresistance in a single-molecule junction, Nat. Commun. **10**, 3599 (2019).

[27] X. Chen, Y.-S. Fu, S.-H. Ji, T. Zhang, P. Cheng, X.-C. Ma, X.-L. Zou, W.-H. Duan, J.-F. Jia, and Q.-K. Xue, Probing superexchange interaction in molecular magnets by spin-flip spectroscopy and microscopy, Phys. Rev. Lett. **101**, 197208 (2008).

[28] N. Tsukahara, K. I. Noto, M. Ohara, S. Shiraki, N. Takagi, Y. Takata, J. Miyawaki, M. Taguchi, A. Chainani, S. Shin, and M. Kawai, Adsorption-induced switching of magnetic anisotropy in a single iron(II) phthalocyanine molecule on an oxidized Cu(110) surface, Phys. Rev. Lett. **102**, 167203 (2009).

[29] T. Choi, W. Paul, S. Rolf-Pissarczyk, A. J. Macdonald, F. D. Natterer, K. Yang, P. Willke, C. P. Lutz, and A. J. Heinrich, Atomic-scale sensing of the magnetic dipolar field from single atoms, Nat. Nanotechnol. **12**, 420 (2017).

[30] F. D. Natterer, K. Yang, W. Paul, P. Willke, T. Choi, T. Greber, A. J. Heinrich, and C. P. Lutz, Reading and writing single-atom magnets, Nature (London) **543**, 226 (2017).

[31] X. Li and J. Yang, First-principles design of spintronics materials, Natl. Sci. Rev. **3**, 365 (2016).

[32] S. Manipatruni, D. E. Nikonov, and I. A. Young, Beyond CMOS computing with spin and polarization, Nat. Phys. **14**, 338 (2018).

[33] A. A. Khajetoorians, D. Wegner, A. F. Otte, and I. Swart, Creating designer quantum states of matter atom-by-atom, Nat. Rev. Phys. **1**, 703 (2019).

[34] F. Delgado and J. Fernández-Rossier, Spin decoherence of magnetic atoms on surfaces, Prog. Surf. Sci. **92**, 40 (2017).

[35] J. Hermenau, M. Ternes, M. Steinbrecher, R. Wiesendanger, and J. Wiebe, Long spin-relaxation times in a transition-metal atom in direct contact to a metal substrate, Nano Lett. **18**, 1978 (2018).

[36] J. Qu and J. Hu, Engineering giant magnetic anisotropy in single-molecule magnets by dimerizing heavy transition-metal atoms, Appl. Phys. Express **11**, 055201 (2018).

[37] D. Jacob, Renormalization of single-ion magnetic anisotropy in the absence of the Kondo effect, Phys. Rev. B **97**, 075428 (2018).

[38] X. Wang, L. Yang, L. Ye, X. Zheng, and Y. Yan, Precise control of local spin states in an adsorbed magnetic molecule with an STM Tip: Theoretical insights from first-principles-based simulation, J. Phys. Chem. Lett. **9**, 2418 (2018).

[39] Y. Wang, X. Li, and J. Yang, Spin-flip excitations induced by dehydrogenation in a magnetic single-molecule junction, J. Chem. Phys. **151**, 224704 (2019).
[40] J. Repp, G. Meyer, S. M. Stojković, A. Gourdon, and C. Joachim, Molecules on insulating films: Scanning-tunneling microscopy imaging of individual molecular orbitals, Phys. Rev. Lett. **94**, 026803 (2005).
[41] W. Paul, K. Yang, S. Baumann, N. Romming, T. Choi, C. P. Lutz, and A. J. Heinrich, Control of the millisecond spin lifetime of an electrically probed atom, Nat. Phys. **13**, 403 (2017).
[42] A. Kumar, K. Banerjee, and P. Liljeroth, Molecular assembly on two-dimensional materials, Nanotechnology **28**, 082001 (2017).
[43] Y. Wang, X. Li, X. Zheng, and J. Yang, Manipulation of spin and magnetic anisotropy in bilayer magnetic molecular junctions, Phys. Chem. Chem. Phys. **20**, 26396 (2018).
[44] T. Schuh, T. Miyamachi, S. Gerstl, M. Geilhufe, M. Hoffmann, S. Ostanin, W. Hergert, A. Ernst, and W. Wulfhekel, Magnetic excitations of rare earth atoms and clusters on metallic surfaces, Nano Lett. **12**, 4805 (2012).
[45] R. Baltic, M. Pivetta, F. Donati, C. Wäckerlin, A. Singha, J. Dreiser, S. Rusponi, and H. Brune, Superlattice of single atom magnets on graphene, Nano Lett. **16**, 7610 (2016).
[46] A. A. Khajetoorians, B. Chilian, J. Wiebe, S. Schuwalow, F. Lechermann, and R. Wiesendanger, Detecting excitation and magnetization of individual dopants in a semiconductor, Nature (London) **467**, 1084 (2010).
[47] B. W. Heinrich, G. Ahmadi, V. L. Müller, L. Braun, J. I. Pascual, and K. J. Franke, Change of the magnetic coupling of a metal-organic complex with the substrate by a stepwise ligand reaction, Nano Lett. **13**, 4840 (2013).
[48] G. R. Bhimanapati, Z. Lin, V. Meunier, Y. Jung, J. Cha, S. Das, D. Xiao, Y. Son, M. S. Strano, V. R. Cooper, L. Liang, S. G. Louie, E. Ringe, W. Zhou, S. S. Kim, R. R. Naik, B. G. Sumpter, H. Terrones, F. Xia, Y. Wang *et al.*, Recent advances in two-dimensional materials beyond graphene, ACS Nano **9**, 11509 (2015).
[49] Y. P. Feng, L. Shen, M. Yang, A. Wang, M. Zeng, Q. Wu, S. Chintalapati, and C.-R. Chang, Prospects of spintronics based on 2D materials, WIREs Comput. Mol. Sci. **7**, e1313 (2017).
[50] S. Yu, J. Tang, Y. Wang, F. Xu, X. Li, and X. Wang, Recent advances in two-dimensional ferromagnetism: strain-, doping-, structural- and electric field-engineering toward spintronic applications, Sci. Technol. Adv. Mater. **23**, 140 (2022).
[51] L. Kong, A. Enders, T. S. Rahman, and P. A. Dowben, Molecular adsorption on graphene, J. Phys.: Condens. Matter **26**, 443001 (2014).
[52] J. M. MacLeod and F. Rosei, Molecular self-assembly on graphene, Small **10**, 1038 (2014).
[53] J.-F. Dayen, S. J. Ray, O. Karis, I. J. Vera-Marun, and M. V. Kamalakar, Two-dimensional van der Waals spinterfaces and magnetic-interfaces, Appl. Phys. Rev. **7**, 011303 (2020).
[54] S. Bhandary, O. Eriksson, and B. Sanyal, Defect controlled magnetism in FeP/graphene/Ni(111), Sci. Rep. **3**, 3405 (2013).
[55] C. F. Hermanns, K. Tarafder, M. Bernien, A. Kroger, Y. M. Chang, P. M. Oppeneer, and W. Kuch, Magnetic coupling of porphyrin molecules through graphene, Adv. Mater. **25**, 3473 (2013).
[56] J. Uihlein, H. Peisert, H. Adler, M. Glaser, M. Polek, R. Ovsyannikov, and T. Chassé, Interface between FePc and Ni(111): Influence of graphene buffer layers, J. Phys. Chem. C **118**, 10106 (2014).
[57] J. Uihlein, M. Polek, M. Glaser, H. Adler, R. Ovsyannikov, M. Bauer, M. Ivanovic, A. B. Preobrajenski, A. V. Generalov, T. Chassé, and H. Peisert, Influence of graphene on charge transfer between CoPc and metals: The role of graphene-substrate coupling, J. Phys. Chem. C **119**, 15240 (2015).
[58] A. Candini, V. Bellini, D. Klar, V. Corradini, R. Biagi, V. De Renzi, K. Kummer, N. B. Brookes, U. del Pennino, H. Wende, and M. Affronte, Ferromagnetic exchange coupling between Fe phthalocyanine and Ni(111) surface mediated by the extended states of graphene, J. Phys. Chem. C **118**, 17670 (2014).
[59] G. Avvisati, C. Cardoso, D. Varsano, A. Ferretti, P. Gargiani, and M. G. Betti, Ferromagnetic and antiferromagnetic coupling of spin molecular interfaces with high thermal stability, Nano Lett. **18**, 2268 (2018).
[60] G. Avvisati, P. Gargiani, P. Mondelli, F. Presel, A. Baraldi, and M. G. Betti, Superexchange pathways stabilize the magnetic coupling of MnPc with Co in a spin interface mediated by graphene, Phys. Rev. B **98**, 115412 (2018).
[61] V. Corradini, A. Candini, D. Klar, R. Biagi, V. De Renzi, A. Lodi Rizzini, N. Cavani, U. del Pennino, H. Wende, E. Otero, and M. Affronte, CoTPP molecules deposited on graphene/Ni (111): Quenching of the antiferromagnetic interaction induced by gold intercalation, J. Appl. Phys. **125**, 142904 (2019).
[62] R. Xu, F. Xuan, and S. Y. Quek, Spin-dependent tunneling barriers in CoPc/VSe_2 from many-body interactions, J. Phys. Chem. Lett. **11**, 9358 (2020).
[63] X. Wang, C. Xiao, C. Yang, M. Chen, S. A. Yang, J. Hu, Z. Ren, H. Pan, W. Zhu, Z.-A. Xu, and Y. Lu, Ferroelectric control of single-molecule magnetism in 2D limit, Sci. Bull. **65**, 1252 (2020).
[64] H. Wende, M. Bernien, J. Luo, C. Sorg, N. Ponpandian, J. Kurde, J. Miguel, M. Piantek, X. Xu, P. Eckhold, W. Kuch, K. Baberschke, P. M. Panchmatia, B. Sanyal, P. M. Oppeneer, and O. Eriksson, Substrate-induced magnetic ordering and switching of iron porphyrin molecules, Nat. Mater. **6**, 516 (2007).
[65] C. Iacovita, M. V. Rastei, B. W. Heinrich, T. Brumme, J. Kortus, L. Limot, and J. P. Bucher, Visualizing the spin of individual cobalt-phthalocyanine molecules, Phys. Rev. Lett. **101**, 116602 (2008).
[66] M. E. Ali, B. Sanyal, and P. M. Oppeneer, Tuning the magnetic interaction between manganese porphyrins and ferromagnetic Co substrate through dedicated control of the adsorption, J. Phys. Chem. C **113**, 14381 (2009).
[67] P. Oppeneer, P. Panchmatia, B. Sanyal, O. Eriksson, and M. Ali, Nature of the magnetic interaction between Fe-porphyrin molecules and ferromagnetic surfaces, Prog. Surf. Sci. **84**, 18 (2009).
[68] J. Girovsky, K. Tarafder, C. Wäckerlin, J. Nowakowski, D. Siewert, T. Hählen, A. Wäckerlin, A. Kleibert, N. Ballav, T. A. Jung, and P. M. Oppeneer, Antiferromagnetic coupling of Cr-porphyrin to a bare Co substrate, Phys. Rev. B **90**, 220404(R) (2014).
[69] T. Kroll, R. Kraus, R. Schönfelder, V. Y. Aristov, O. V. Molodtsova, P. Hoffmann, and M. Knupfer, Transition metal phthalocyanines: Insight into the electronic structure from soft x-ray spectroscopy, J. Chem. Phys. **137**, 054306 (2012).

[70] A. Mugarza, R. Robles, C. Krull, R. Korytár, N. Lorente, and P. Gambardella, Electronic and magnetic properties of molecule-metal interfaces: Transition-metal phthalocyanines adsorbed on Ag(100), Phys. Rev. B **85**, 155437 (2012).

[71] A. J. Wallace, B. E. Williamson, and D. L. Crittenden, CASSCF-based explicit ligand field models clarify the ground state electronic structures of transition metal phthalocyanines (MPc; M = Mn, Fe, Co, Ni, Cu, Zn), Can. J. Chem. **94**, 1163 (2016).

[72] S. C. Matysik, C. Papp, and A. Görling, Solving the puzzle of the coexistence of different adsorption geometries of graphene on Ni(111), J. Phys. Chem. C **122**, 26105 (2018).

[73] E. Annese, F. Casolari, J. Fujii, and G. Rossi, Interface magnetic coupling of Fe-phthalocyanine layers on a ferromagnetic surface, Phys. Rev. B **87**, 054420 (2013).

[74] F. Bianchini, L. L. Patera, M. Peressi, C. Africh, and G. Comelli, Atomic scale identification of coexisting graphene structures on Ni(111), J. Phys. Chem. Lett. **5**, 467 (2014).

[75] A. Barla, V. Bellini, S. Rusponi, P. Ferriani, M. Pivetta, F. Donati, F. Patthey, L. Persichetti, S. K. Mahatha, M. Papagno, C. Piamonteze, S. Fichtner, S. Heinze, P. Gambardella, H. Brune, and C. Carbone, Complex magnetic exchange coupling between Co nanostructures and Ni(111) across epitaxial graphene, ACS Nano **10**, 1101 (2016).

[76] Z. Hu, B. Li, A. Zhao, J. Yang, and J. G. Hou, Electronic and magnetic properties of metal phthalocyanines on Au(111) surface: A first-principles study, J. Phys. Chem. C **112**, 13650 (2008).

[77] Y. Y. Zhang, S. X. Du, and H.-J. Gao, Binding configuration, electronic structure, and magnetic properties of metal phthalocyanines on a Au(111) surface studied with *ab initio* calculations, Phys. Rev. B **84**, 125446 (2011).

[78] P. E. Blöchl, Projector augmented-wave method, Phys. Rev. B **50**, 17953 (1994).

[79] G. Kresse and J. Hafner, Norm-conserving and ultrasoft pseudopotentials for first-row and transition elements, J. Phys.: Condens. Matter **6**, 8245 (1994).

[80] J. P. Perdew, K. Burke, and M. Ernzerhof, Generalized gradient approximation made simple, Phys. Rev. Lett. **77**, 3865 (1996).

[81] S. Grimme, J. Antony, S. Ehrlich, and H. Krieg, A consistent and accurate *ab initio* parametrization of density functional dispersion correction (DFT-D) for the 94 elements H-Pu, J. Chem. Phys. **132**, 154104 (2010).

[82] S. Grimme, S. Ehrlich, and L. Goerigk, Effect of the damping function in dispersion corrected density functional theory, J. Comput. Chem. **32**, 1456 (2011).

[83] S. Haldar, S. Bhandary, H. Vovusha, and B. Sanyal, Comparative study of electronic and magnetic properties of iron and cobalt phthalocyanine molecules physisorbed on two-dimensional MoS_2 and graphene, Phys. Rev. B **98**, 085440 (2018).

[84] Y. Wang, X. Li, and J. Yang, Electronic and magnetic properties of CoPc and FePc molecules on graphene: the substrate, defect, and hydrogen adsorption effects, Phys. Chem. Chem. Phys. **21**, 5424 (2019).

[85] Y. Wang, Z. Wang, J. Yang, and X. Li, Precise spin manipulation of single molecule positioning on graphene by coordination chemistry, J. Phys. Chem. Lett. **11**, 9819 (2020).

[86] S. L. Dudarev, G. A. Botton, S. Y. Savrasov, C. J. Humphreys, and A. P. Sutton, Electron-energy-loss spectra and the structural stability of nickel oxide: An LSDA+U study, Phys. Rev. B **57**, 1505 (1998).

[87] D. Klar, B. Brena, H. C. Herper, S. Bhandary, C. Weis, B. Krumme, C. Schmitz-Antoniak, B. Sanyal, O. Eriksson, and H. Wende, Oxygen-tuned magnetic coupling of Fe-phthalocyanine molecules to ferromagnetic Co films, Phys. Rev. B **88**, 224424 (2013).

[88] J. Tong, F. Luo, L. Ruan, G. Liu, L. Zhou, F. Tian, G. Qin, and X. Zhang, Interfacial antiferromagnetic coupling and high spin polarization in metallic phthalocyanines, Phys. Rev. B **103**, 024435 (2021).

[89] K. Nakamura, Y. Kitaoka, T. Akiyama, T. Ito, M. Weinert, and A. J. Freeman, Constraint density functional calculations for multiplets in a ligand-field applied to Fe-phthalocyanine, Phys. Rev. B **85**, 235129 (2012).

[90] M. D. Kuz'min, A. Savoyant, and R. Hayn, Ligand field parameters and the ground state of Fe(II) phthalocyanine, J. Chem. Phys. **138**, 244308 (2013).

[91] I. E. Brumboiu, R. Totani, M. de Simone, M. Coreno, C. Grazioli, L. Lozzi, H. C. Herper, B. Sanyal, O. Eriksson, C. Puglia, and B. Brena, Elucidating the 3*d* electronic configuration in manganese phthalocyanine, J. Phys. Chem. A **118**, 927 (2014).

[92] V. I. Anisimov, J. Zaanen, and O. K. Andersen, Band theory and mott insulators: Hubbard U instead of stoner I, Phys. Rev. B **44**, 943 (1991).

[93] A. I. Liechtenstein, V. I. Anisimov, and J. Zaanen, Density-functional theory and strong interactions: Orbital ordering in mott-hubbard insulators, Phys. Rev. B **52**, R5467 (1995).

[94] B. Dorado, B. Amadon, M. Freyss, and M. Bertolus, DFT + U calculations of the ground state and metastable states of uranium dioxide, Phys. Rev. B **79**, 235125 (2009).

[95] G. Trimarchi, Z. Wang, and A. Zunger, Polymorphous band structure model of gapping in the antiferromagnetic and paramagnetic phases of the Mott insulators MnO, FeO, CoO, and NiO, Phys. Rev. B **97**, 035107 (2018).

[96] J. P. Allen and G. W. Watson, Occupation matrix control of d- and f-electron localisations using DFT+U, Phys. Chem. Chem. Phys. **16**, 21016 (2014).

[97] B. Meredig, A. Thompson, H. A. Hansen, C. Wolverton, and A. van de Walle, Method for locating low-energy solutions within DFT + U, Phys. Rev. B **82**, 195128 (2010).

[98] E. Minamitani, N. Tsukahara, D. Matsunaka, Y. Kim, N. Takagi, and M. Kawai, Symmetry-driven novel kondo effect in a molecule, Phys. Rev. Lett. **109**, 086602 (2012).

[99] Y. Wang, X. Zheng, and J. Yang, Environment-modulated Kondo phenomena in FePc/Au(111) adsorption systems, Phys. Rev. B **93**, 125114 (2016).

[100] N. Marom and L. Kronik, Density functional theory of transition metal phthalocyanines, II: electronic structure of MnPc and FePc–symmetry and symmetry breaking, Appl. Phys. A **95**, 165 (2009).

[101] B. Brena, C. Puglia, M. de Simone, M. Coreno, K. Tarafder, V. Feyer, R. Banerjee, E. Göthelid, B. Sanyal, P. M. Oppeneer, and O. Eriksson, Valence-band electronic structure of iron phthalocyanine: An experimental and theoretical photoelectron spectroscopy study, J. Chem. Phys. **134**, 074312 (2011).

[102] C. J. Stein and M. Reiher, Automated selection of active orbital spaces, J. Chem. Theory Comput. **12**, 1760 (2016).

[103] A. L. Wysocki and K. Park, Nature of hyperfine interactions in $TbPc_2$ single-molecule magnets: Multiconfigurational *ab initio* study, Inorg. Chem. **59**, 2771 (2020).

[104] Z. Tóth and P. Pulay, Comparison of methods for active orbital selection in multiconfigurational calculations, J. Chem. Theory Comput. **16**, 7328 (2020).

[105] J. Brede, N. Atodiresei, S. Kuck, P. Lazić, V. Caciuc, Y. Morikawa, G. Hoffmann, S. Blügel, and R. Wiesendanger, Spin- and energy-dependent tunneling through a single molecule with intramolecular spatial resolution, Phys. Rev. Lett. **105**, 047204 (2010).

[106] S. Marocchi, P. Ferriani, N. M. Caffrey, F. Manghi, S. Heinze, and V. Bellini, Graphene-mediated exchange coupling between a molecular spin and magnetic substrates, Phys. Rev. B **88**, 144407 (2013).

[107] X. Chen and M. Alouani, Effect of metallic surfaces on the electronic structure, magnetism, and transport properties of Co-phthalocyanine molecules, Phys. Rev. B **82**, 094443 (2010).

[108] A. Jaafar, I. Rungger, S. Sanvito, and M. Alouani, Effect of a ferromagnetic STM cobalt tip on a single Co-phthalocyanine molecule adsorbed on a ferromagnetic substrate, Phys. Open **9**, 100088 (2021).

[109] F. Ellinger, C. Franchini, and V. Bellini, Magnetic 3*d* adatoms on free-standing and Ni(111)-supported graphene, Phys. Rev. Mater. **5**, 014406 (2021).

[110] J. Åhlund, J. Schnadt, K. Nilson, E. Göthelid, J. Schiessling, F. Besenbacher, N. Mårtensson, and C. Puglia, The adsorption of iron phthalocyanine on graphite: A scanning tunnelling microscopy study, Surf. Sci. **601**, 3661 (2007).

[111] S. Bhandary, E. Poli, G. Teobaldi, and D. D. O'Regan, Dynamical screening of local spin moments at metal-molecule interfaces, ACS Nano **17**, 5974 (2023).

[112] W. Dou, S. Huang, R. Q. Zhang, and C. S. Lee, Molecule-substrate interaction channels of metal-phthalocyanines on graphene on Ni(111) surface, J. Chem. Phys. **134**, 094705 (2011).

[113] S. Javaid, M. Bowen, S. Boukari, L. Joly, J.-B. Beaufrand, X. Chen, Y. J. Dappe, F. Scheurer, J.-P. Kappler, J. Arabski, W. Wulfhekel, M. Alouani, and E. Beaurepaire, Impact on interface spin polarization of molecular bonding to metallic surfaces, Phys. Rev. Lett. **105**, 077201 (2010).

[114] V. Wang, N. Xu, J.-C. Liu, G. Tang, and W.-T. Geng, VASPKIT: A user-friendly interface facilitating high-throughput computing and analysis using VASP code, Comput. Phys. Commun. **267**, 108033 (2021).

[115] K. Momma and F. Izumi, VESTA 3 for three-dimensional visualization of crystal, volumetric and morphology data, J. Appl. Crystallogr. **44**, 1272 (2011).

[116] See Supplemental Material at http://link.aps.org/supplemental/10.1103/PhysRevB.109.014428 for the details of calculation for magnetic couplings, electronic structure analysis and the mechanism of magnetic couplings in TMPc/Ni(111) and TMPc/Gr/Ni(111) (TM=Cr, Mn and Fe) composites, which contains Refs. [117–119].

[117] G. Filoti, M. D. Kuz'min, and J. Bartolomé, Mössbauer study of the hyperfine interactions and spin dynamics in α-iron(II) phthalocyanine, Phys. Rev. B **74**, 134420 (2006).

[118] M. D. Kuz'min, R. Hayn, and V. Oison, *ab initio* calculated XANES and XMCD spectra of Fe(II) phthalocyanine, Phys. Rev. B **79**, 024413 (2009).

[119] S. Stepanow, P. S. Miedema, A. Mugarza, G. Ceballos, P. Moras, J. C. Cezar, C. Carbone, F. M. F. de Groot, and P. Gambardella, Mixed-valence behavior and strong correlation effects of metal phthalocyanines adsorbed on metals, Phys. Rev. B **83**, 220401(R) (2011).

[120] A. Lodi Rizzini, C. Krull, A. Mugarza, T. Balashov, C. Nistor, R. Piquerel, S. Klyatskaya, M. Ruben, P. M. Sheverdyaeva, P. Moras, C. Carbone, C. Stamm, P. S. Miedema, P. K. Thakur, V. Sessi, M. Soares, F. Yakhou-Harris, J. C. Cezar, S. Stepanow, and P. Gambardella, Coupling of single, double, and triple-decker metal-phthalocyanine complexes to ferromagnetic and antiferromagnetic substrates, Surf. Sci. **630**, 361 (2014).

[121] A. Scheybal, T. Ramsvik, R. Bertschinger, M. Putero, F. Nolting, and T. A. Jung, Induced magnetic ordering in a molecular monolayer, Chem. Phys. Lett. **411**, 214 (2005).

[122] D. Chylarecka, T. K. Kim, K. Tarafder, K. Müller, K. Gödel, I. Czekaj, C. Wäckerlin, M. Cinchetti, M. E. Ali, C. Piamonteze, F. Schmitt, J.-P. Wüstenberg, C. Ziegler, F. Nolting, M. Aeschlimann, P. M. Oppeneer, N. Ballav, and T. A. Jung, Indirect magnetic coupling of manganese porphyrin to a ferromagnetic cobalt substrate, J. Phys. Chem. C **115**, 1295 (2011).

[123] M. Bernien, J. Miguel, C. Weis, M. E. Ali, J. Kurde, B. Krumme, P. M. Panchmatia, B. Sanyal, M. Piantek, P. Srivastava, K. Baberschke, P. M. Oppeneer, O. Eriksson, W. Kuch, and H. Wende, Tailoring the nature of magnetic coupling of fe-porphyrin molecules to ferromagnetic substrates, Phys. Rev. Lett. **102**, 047202 (2009).

[124] D. Chylarecka, C. Wäckerlin, T. K. Kim, K. Müller, F. Nolting, A. Kleibert, N. Ballav, and T. A. Jung, Self-assembly and superexchange coupling of magnetic molecules on oxygen-reconstructed ferromagnetic thin film, J. Phys. Chem. Lett. **1**, 1408 (2010).

[125] A. Lodi Rizzini, C. Krull, T. Balashov, J. J. Kavich, A. Mugarza, P. S. Miedema, P. K. Thakur, V. Sessi, S. Klyatskaya, M. Ruben, S. Stepanow, and P. Gambardella, Coupling single molecule magnets to ferromagnetic substrates, Phys. Rev. Lett. **107**, 177205 (2011).

[126] Y.-S. Fu, Q.-K. Xue, and R. Wiesendanger, Spin-resolved splitting of kondo resonances in the presence of RKKY-type coupling, Phys. Rev. Lett. **108**, 087203 (2012).

[127] C. Wäckerlin, D. Chylarecka, A. Kleibert, K. Müller, C. Iacovita, F. Nolting, T. A. Jung, and N. Ballav, Controlling spins in adsorbed molecules by a chemical switch, Nat. Commun. **1**, 61 (2010).

[128] A. Swain, T. Sharma, and G. Rajaraman, Strategies to quench quantum tunneling of magnetization in lanthanide single molecule magnets, Chem. Commun. **59**, 3206 (2023).

[129] A. Dahal and M. Batzill, Graphene-nickel interfaces: a review, Nanoscale **6**, 2548 (2014).

[130] J. B. Goodenough, *Magnetism and the Chemical Bond* (Wiley, New York, 1963).

[131] R. López and D. Sánchez, Nonequilibrium spintronic transport through an artificial kondo impurity: Conductance, magnetoresistance, and shot noise, Phys. Rev. Lett. **90**, 116602 (2003).

[132] A. N. Pasupathy, The kondo effect in the presence of ferromagnetism, Science **306**, 86 (2004).

[133] J. Martinek, M. Sindel, L. Borda, J. Barnaś, J. König, G. Schön, and J. von Delft, Kondo effect in the presence of itinerant-electron ferromagnetism studied with the numerical renormalization group method, Phys. Rev. Lett. **91**, 247202 (2003).

[134] S. L. Kawahara, J. Lagoute, V. Repain, C. Chacon, Y. Girard, J. Klein, and S. Rousset, Kondo peak splitting on a single adatom coupled to a magnetic cluster, Phys. Rev. B **82**, 020406(R) (2010).

[135] Y. Li, A. T. Ngo, A. DiLullo, K. Z. Latt, H. Kersell, B. Fisher, P. Zapol, S. E. Ulloa, and S.-W. Hla, Anomalous Kondo resonance mediated by semiconducting graphene nanoribbons in a molecular heterostructure, Nat. Commun. **8**, 946 (2017).

[136] G. D. Scott and T.-C. Hu, Gate-controlled Kondo effect in a single-molecule transistor with elliptical ferromagnetic leads, Phys. Rev. B **96**, 144416 (2017).

[137] B. de la Torre, M. Švec, P. Hapala, J. Redondo, O. Krejčí, R. Lo, D. Manna, A. Sarmah, D. Nachtigallová, J. Tuček, P. Błoński, M. Otyepka, R. Zbořil, P. Hobza, and P. Jelínek, Non-covalent control of spin-state in metal-organic complex by positioning on N-doped graphene, Nat. Commun. **9**, 2831 (2018).

[138] M. Bouatou, R. Harsh, F. Joucken, C. Chacon, V. Repain, A. Bellec, Y. Girard, S. Rousset, R. Sporken, F. Gao, M. Brandbyge, Y. J. Dappe, C. Barreteau, A. Smogunov, and J. Lagoute, Intraconfigurational transition due to surface-induced symmetry breaking in noncovalently bonded molecules, J. Phys. Chem. Lett. **11**, 9329 (2020).

[139] Y. Wang, S. Arabi, K. Kern, and M. Ternes, Symmetry mediated tunable molecular magnetism on a 2D material, Commun. Phys. **4**, 103 (2021).

[140] R. Drost, S. Kezilebieke, J. L. Lado, and P. Liljeroth, Real-space imaging of triplon excitations in engineered quantum magnets, Phys. Rev. Lett. **131**, 086701 (2023).

[141] L. Fritz and M. Vojta, The physics of Kondo impurities in graphene, Rep. Prog. Phys. **76**, 032501 (2013).

[142] J. Ren, H. Guo, J. Pan, Y. Y. Zhang, X. Wu, H.-G. Luo, S. Du, S. T. Pantelides, and H.-J. Gao, Kondo effect of cobalt adatoms on a graphene monolayer controlled by substrate-induced ripples, Nano Lett. **14**, 4011 (2014).

[143] B. Yan, X. Li, J. Zhao, Z. Jia, F. Tang, Z. Zhang, D. Yu, K. Liu, L. Zhang, and X. Wu, Gate tunable Kondo effect in magnetic molecule decorated graphene, Solid State Commun. **278**, 24 (2018).

[144] D.-J. Choi, M. V. Rastei, P. Simon, and L. Limot, Conductance-driven change of the kondo effect in a single cobalt atom, Phys. Rev. Lett. **108**, 266803 (2012).